

Establishment of Input Large-scale Earthquake Motions for Earthquake-proof Evaluation of Existing Dams

by

Nario Yasuda¹, Kazuhito Shimamoto², Takayuki Sano³, Kohji Sujino⁴

ABSTRACT

In March 2005, the River Bureau of the Ministry of Land, Infrastructure and Transport issued the “Guidelines for Seismic Safety Evaluation of Dams (draft) and Explanation.”

In establishing the earthquake motion for evaluating the seismic performance of dams against large-scale earthquakes, the earthquakes considered likely to have the greatest impact on the dam site (Scenario earthquakes) shall be selected based on information such as past earthquakes and relevant active faults, and then earthquake motions shall be estimated for the dam site.

There are several methods for establishing earthquake motion at a dam site, such as attenuation relationships for dams which are empirical and based on records of earthquake motions at the dam site, and statistical Green's function method which is semi-empirical.

This report describes the specific procedure for establishing large-scale earthquake motion at existing dam sites, and compares the earthquake motions predicted by several methods.

KEYWORDS: dam, large-scale earthquake, seismic performance, Level 2 earthquake motion, attenuation relationships, statistical Green's function method

1. INTRODUCTION

Large earthquake disasters have occurred since the 1995 Hyogoken-Nanbu Earthquake more than ten years ago, and a large earthquake is likely to occur in the near future. Thus, there is growing concern for the safety of infrastructures during a large earthquake.

In relation to dams, in March 2005, the River

Bureau of the Ministry of Land, Infrastructure and Transport issued the “Guidelines for Seismic Safety Evaluation of Dams (draft) and Explanation” (hereafter, “Draft Guidelines”) [1] which describe methods for evaluating the seismic performance of dams against large-scale earthquakes, assuming Level 2 earthquake motions.

In the Draft Guidelines, Level 2 earthquake motions are defined as “the strongest seismic ground motion potentially expected at a given dam site at present and in the foreseeable future,” which follows the definition given in Phase 3 Recommendations [2] announced by the Japan Society of Civil Engineers immediately after the 1995 Hyogoken-Nanbu Earthquake.

This report describes the specific procedure for establishing large-scale earthquake motion (Level 2 earthquake motion) at N Dam, and compares the earthquake motions predicted by several methods. Figure 1 shows the outline of the method for establishing Level 2 earthquake motion. The process is explained below based on this figure.

-
- 1) Head, Water Management and Dam Division (WMDD), National Institute for Land and Infrastructure Management (NILIM), Ministry of Land, Infrastructure and Transport (MLIT), 1, Asahi, Tsukuba, Ibaraki, 305-0804, Japan
 - 2) Senior Researcher, ditto
 - 3) Researcher, ditto
 - 4) Assistant section head, Electricity Infrastructure Division, Agency for Natural Resources and Energy Electricity and Gas Industry Department, Ministry of Economy, Trade and Industry, 1-3-1, Kasumigaseki, Chiyoda-ku, Tokyo, 100-8931, Japan (Former : Senior Researcher, WMDD, NILIM, MLIT)

2. CASE STUDY OF ESTABLISHING LEVEL 2 EARTHQUAKE MOTION

2.1 Selection of Scenario earthquakes

2.1.1 Literature review

First, data on active faults and seismic faults at plate boundaries that were likely to induce ground motions greatly affecting N Dam and on past earthquakes that had caused damages were compiled from literature including published results of existing studies. Documents included a revised edition of "Active faults in Japan", "Fault scarp parameter handbook for Japan", "Detailed digital map of active faults", "Metropolitan area active fault map", a revised edition of "Damage-inducing earthquakes of Japan", materials of the "Central Disaster Prevention Council" and materials of the "Headquarters for Earthquake Research Promotion". The results of surveys of Quaternary faults at and near dam sites were also used. Figure 2 shows the results of the investigation.

Secondly, data were extracted on faults that were generally within 50 km of the dam site. Even for faults that were more than 50 km away from the dam site, the fault was examined when a Scenario earthquake with a magnitude of 8 or higher is expected to occur at the fault. This work extracted various kinds of earthquakes and faults as shown in Table 1.

2.1.2 Selection of Scenario earthquakes

Among the various earthquakes listed in Table 1, the earthquakes that would likely have the greatest impact on N Dam were selected as the Scenario earthquakes.

The Scenario earthquakes were selected by presuming the intensity (acceleration response spectrum) of the seismic ground motion caused at the dam site by using attenuation relationships as described later.

Figure 3 shows the acceleration response spectra of the earthquake motion at the dam site due to various earthquakes, which were obtained by attenuation relationships. Figure 3 (a) is the result using the shortest distance equation, and

Fig. 3 (b) is the result using the equivalent distance equation.

Based on Fig. 3, the earthquake caused by the Median tectonic line Akaishi-sanchi-seien fault zone, which is an inland type, and the anticipated Tokai Earthquake, which is an ocean type, were selected as the Scenario earthquakes at N Dam. When selecting the Scenario earthquakes, comparison was made by taking into account not only acceleration response spectra but also factors such as the type and duration of the earthquake.

2.2 Establishing Level 2 earthquake motion for evaluating the seismic performance of dams

2.2.1 Estimation of earthquake motions due to Scenario earthquakes

We estimated the earthquake motions at the N Dam site due to the Scenario earthquakes. In this study, we used empirical attenuation relationships based on earthquake motions recorded at the dam site, and the statistical Green's function method.

The processes of the estimations are explained below.

(1) Estimation of earthquake motions by empirical method

We estimated the acceleration response spectra of earthquake motion at the N Dam site due to the Scenario earthquakes using attenuation relationships.

Attenuation relationships for estimating earthquake motions have been developed based on numerous records of earthquake motions with respect to dam foundations in Japan. With these formulas, it is possible to estimate the intensity of earthquake motions at a particular dam site (acceleration response spectra) using distance from hypocenter, magnitude of earthquake and coefficients for individual types.

Acceleration response spectra of earthquake motions produced in ground (with an average shear wave velocity of approximately 0.7–1.5 km/s) that can serve as the dam foundation were estimated by attenuation relationships. Namely,

these relationships were obtained as regression equations by performing statistical analysis as follows: Earthquake records were obtained from strong motion seismographs installed at locations such as in the bottom inspection galleries of dams. Statistical analysis was conducted with respect to acceleration response spectra values (mean values plus standard deviations) for parameters such as: shortest distance to fault plane, earthquake magnitude, and depth from ground surface to fault plane center.

There are two formulas depending on how the distance from the hypocenter is measured: the shortest distance formula (Eq. 1) in which the shortest distance between the fault plane and dam site is used, and the equivalent distance formula (Eq. 2) in which the distance between the dam site and virtual point source where seismic energy is equivalent to that from fault planes is used.[3][4]

$$\log S_A (T) = C_m (T) M + C (T) H_c - C_d (T) \log \{R + 0.334 \exp (0.653M)\} + C_o (T) \quad (1)$$

$$\log S_A (T) = C_m (T) M + C_h (T) H_c - C_d (T) X_{eq} - \log X_{eq} + C_o (T) \quad (2)$$

where,

T: Characteristic period

$S_A (T)$: Average response spectra of two horizontal components

M: Magnitude (Japan Meteorological Agency magnitude) of earthquake occurring on a fault

H_c : Depth of fault plane center from ground surface, or 100 km, whichever is less

R: Shortest distance to fault plane

X_{eq} : Equivalent hypocentral distance

$C_m (T)$, $C_h (T)$, $C_d (T)$, and $C_o (T)$:

Regression coefficients obtained from numerous earthquake records.

In order to estimate earthquake motions by using attenuation relationships, it is necessary to establish specific distances between the dam site and faults (R or X_{eq}), magnitude of earthquakes occurring on faults (M), and depth of fault plane centers from ground surface (H_c).

Of these variables, the following values can

be calculated based on the literature, provided that the locations of fault planes are known.

Regarding the magnitude (M) of earthquakes occurring on faults, in cases where relevant values are shown in the literature, then such values can be used. However, if only the lengths of faults are known, then the magnitudes of earthquakes that occur when pertinent faults are triggered can be estimated by using formulas such as relational equations empirically obtained between fault length and fault width or between fault area and earthquake magnitude.

Earthquake caused by Median tectonic line Akaishi-sanchi-seien fault zone

The locations of the Median tectonic line Akaishi-sanchi-seien fault zone and N Dam site are shown in Fig. 4, and the fault parameters of the Akaishi-sanchi-seien fault zone are shown in Table 2. Figure 5 shows the acceleration response spectra at the N Dam site estimated by using attenuation relationships for dams based on the parameter. This figure shows that the spectrum which is estimated by the equivalent distance equation is covered by the spectrum which is estimated by the shortest distance equation.

Anticipated Tokai Earthquake

As for earthquake motion due to the anticipated Tokai Earthquake, the Central Disaster Prevention Council has published acceleration time-history waveforms estimated by the statistical Green's function method.

(2) Estimation of earthquake motions by semi-empirical method

We estimated the acceleration time-history waveforms of earthquake motion at the N Dam site due to the Scenario earthquakes by using a semi-empirical method.

The semi-empirical method synthesizes the waveform of a large earthquake from the waveform of an existing small earthquake. There are two approaches: the empirical Green's function method and the statistical Green's function method.

The empirical Green's function method

synthesizes an element wave (Green's function) according to the destruction process of the assumed fault. An element wave is the waveform of a small and medium-sized earthquake that occurs in the hypocentral region of the assumed fault. The time-history of the waveform can be predicted, and the influence of the destruction process and the influence of asperity can be considered. However, it is necessary to have obtained an appropriate observation waveform beforehand at the evaluation point.

In the statistical Green's function method, the waveform with the average characteristic of many observed earthquake motions is used as an element wave, and so a suitable observed motion at the evaluation point is not needed. However, the vibration corresponding to a characteristic peculiar to the evaluation point is not reflected easily. The time-history of the waveform is calculated by a method similar to the empirical Green's function method.

Earthquake caused by Median tectonic line Akaishi-sanchi-seien fault zone

Because there is no record of earthquake motion caused by the Akaishi-sanchi-seien fault zone, we used the statistical Green's function method.

The estimation procedure using this method is as follows.

Green's functions are created on the seismic base (shear wave velocity: approximately 3000 m/s) considering the characteristics of the epicenter and wave propagation path. The functions are converted to Green's functions on the engineering base (shear wave velocity: approximately 700 m/s) using one-dimensional multiple reflection theory. Strong ground motion is synthesized on the engineering base by convoluting Green's functions on the engineering base.

Causative fault parameters were basically established according to a "recipe" for predicting strong ground motion published by the Headquarters for Earthquake Research Promotion [5]. Table 3 lists the causative fault parameters established for calculation.

Establishing the locations of asperities and rupture starting points involves numerous uncertainties such as the quantities and locations of these parameters, and so predictions of seismic ground motions vary greatly. In this study, dozens of locations were assumed for asperities and rupture starting points (Fig. 6), and the acceleration time-history waveform and response spectra were calculated by applying the statistical Green's function method in 108 cases. A spectrum with a 90% probability of not exceeding the calculated spectra is shown in Fig. 7.

Anticipated Tokai Earthquake

Figure 8 shows the position of the anticipated Tokai Earthquake and N Dam site.

It is difficult to predict the earthquake motion by the empirical Green's function method, because there is no observation record of motion at the N Dam site relating to earthquakes in the focal region of the Tokai Earthquake.

On the other hand, regarding the anticipated Tokai Earthquake, the Central Disaster Prevention Council [6] has published time-history waveforms of earthquake motions on the engineering base (shear wave velocity: approximately 700 m/s) calculated by the statistical Green's function method for each 1 square km.

As a dam foundation generally has a shear wave velocity of 0.7–1.5 km/s and is considered to be equivalent to the engineering base, we adopted the waveform at the N Dam site given by the Central Disaster Prevention Council as the estimated waveform for the foundation of N Dam.

Furthermore, due to the expression of stress reduction in two models (the S model) having different rupture starting points have been published: the S-1 model and S-2 model. The acceleration time-history waveform was estimated by using these fault models and the statistical Green's function method. Figure 9 shows the acceleration response spectra of those waveforms. This figure shows that the spectrum estimated by the S-1 model is almost covered by the spectrum estimated by the S-2 model.

2.2.2 Comparisons with earthquake motions observed in the past and those having lower-limit acceleration response spectrum for evaluation

(1) Comparison with earthquake motions observed in the past

The earthquake motions observed at and near the dam site were sufficiently small in comparison with earthquake motions with lower-limit acceleration response spectrum for evaluation. Therefore, the earthquake motions in the past would not have had the greatest impact on N Dam.

(2) Comparison with earthquake motions having lower-limit acceleration response spectrum for evaluation

(2)-1 Explanation of lower-limit acceleration response spectra for evaluation

The standard practice for establishing Level 2 earthquake motions is to use earthquake motions at dam sites based on Scenario earthquakes. However, in cases where active faults on which hypocenters may be located are not detected in surrounding areas, then the distances to the hypocenters of Scenario earthquakes turn out to be long, and so earthquake motions at the dam site are small.

On the other hand, there is intense seismic activity in Japan, so even if no active faults are detected on the ground surface, they may exist under the ground. The Draft Guidelines specify the following: Even if active faults on which earthquake hypocenters are located are not detected on the ground surface, it shall be assumed that there is a risk of occurrence of earthquakes of certain magnitudes. The acceleration response spectra shown in Fig. 10 shall be referred to as “lower-limit acceleration response spectra for evaluation.” Even in cases where earthquake motions based on Scenario earthquakes are below these limit values, earthquake motions of these levels must be taken into account for evaluation as the lower limit.

As shown in the Recommendations of the

Japan Society of Civil Engineers, earthquakes exceeding a magnitude of M6.5 often leave some sort of mark on the ground surface. Lower-limit acceleration response spectra for evaluation were set as follows: Earthquake motions that occur on ground surfaces during an earthquake with a magnitude of M6.5 directly under a dam site were calculated on a trial basis using tools such as attenuation relationships. To be on the safe side, standard deviations were added to averages. Acceleration response spectra were set such that the results thus calculated were safely covered and the effects of response characteristics (characteristic period bands) were taken into account.

In the 2000 Western Tottori Earthquake (M7.3), which occurred in October 2000, the active fault on which the hypocenter was located had not been known to exist. Views differ among experts as to whether or not this active fault would have been detected if detailed investigations had been made beforehand. However, this case actually occurred, and so the following was also performed: a trial calculation was made by taking into account an earthquake of the same magnitude (M7.3) located directly above the hypocenter, and the results confirmed that the lower-limit acceleration response spectra set as mentioned above safely enveloped the average levels of estimated earthquake motions caused by an earthquake of M7.3.

(2)-2 Comparison

The acceleration response spectra of the earthquake motion at the N Dam site calculated by the empirical and semi-empirical methods were compared with the lower-limit acceleration response spectrum for evaluation. The results are shown in Fig. 11.

As for the earthquake due to the Akaishi-sanchi-seien fault zone, the spectrum estimated by attenuation relationships (equivalent distance equation) and by statistical Green’s function (specifically, a spectrum with a 90% probability of not exceeding the calculated spectrum) are almost covered by the lower-limit acceleration response spectrum for evaluation. Furthermore, a spectrum with a 90% probability of not exceeding the calculated spectrum is

almost covered by the spectrum estimated by attenuation relationships (equivalent distance equation).

Comparing the spectra due to the anticipated Tokai Earthquake (S-2 model) and the lower-limit acceleration response spectrum for evaluation, it is not clear which is the larger.

In view of the above, the earthquake motion due to the anticipated Tokai Earthquake (S-2 model) and the earthquake motion with the lower-limit acceleration response spectrum for evaluation were selected as the earthquake motions that are likely to have the greatest impact on the N Dam.

2.2.3 Preparation of time-history waveform corresponding to acceleration response spectrum

We used the acceleration time-history waveform of earthquake motion selected in the previous section as the level 2 earthquake motion for evaluation.

(1) Earthquake motion due to the anticipated Tokai Earthquake (S-2 model)

For this earthquake, we adopted the waveform published by the Central Disaster Prevention Council. For dynamic analysis, we converted the horizontal components to the directions of the dam by linear transformation. Figure 12(a) shows the waveform after conversion.

(2) Earthquake motion with the lower-limit acceleration response spectrum for evaluation

We prepared the acceleration time-history waveform of earthquake motion with the lower-limit acceleration response spectrum for evaluation.

The phase characteristic was given by the recorded acceleration time-history waveform. In this study, we adopted the waveform observed at the foundation of Hitokura Dam and Gongen Dam in the 1995 Hyogoken-Nanbu Earthquake as the strong records. By adjusting the frequency characteristic of the waveform, we then derived the acceleration time-history waveforms (Fig. 12 (b) and (c)).

From the above, the acceleration time-history waveforms shown in Fig. 12(a)–(c) were established as the level 2 earthquake motions of N Dam.

3. CONCLUSIONS

This report described the specific procedure for establishing large-scale earthquake motion (Level 2 earthquake motion) at N Dam as follows:

1. Data on active faults and seismic faults at plate boundaries that were likely to induce ground motions greatly affecting N Dam and on past earthquakes that had caused damages were compiled from literature including published results of existing studies.
2. The Scenario earthquakes were selected by presuming the intensity (acceleration response spectrum) of the earthquake motion caused at the dam site by using attenuation relationships. As the Scenario earthquakes at N Dam, the earthquake caused by the Median tectonic line Akaishi-sanchi-seien fault zone, which is an inland type earthquake, and the anticipated Tokai Earthquake, which is an ocean type earthquake, were selected.
3. The earthquake motions at the N Dam site due to Scenario earthquakes were estimated by empirical attenuation relationships and based on records of earthquake motions at the dam site, and the statistical Green's function method.
4. To select the earthquake motions that are likely to have the greatest impact on N Dam, the earthquake motions caused by the Scenario earthquakes were compared with the earthquake motions observed in the past, and earthquake motions with the lower-limit acceleration response spectrum for evaluation. As a result, the earthquake motion due to the anticipated Tokai Earthquake (S-2 model) and the earthquake motion with the lower-limit acceleration response spectrum for evaluation were selected as Level 2 earthquake motions.

4. REFERENCES

- 1) Flood Control Division, River Bureau, Ministry of Land, Infrastructure and Transport, "Draft Guidelines for Seismic Safety Evaluation of Dams Subjected to Large-Scale Earthquakes," March 2005 (in Japanese)
- 2) Japan Society of Civil Engineers (Ad Hoc Committee on Methods of Earthquake Resistant Design of Civil Engineering Structures), "Phase 3 Recommendations on Matters Including Seismic Performance and Methods of Earthquake Resistant Design of Civil Engineering Structures," 2000
- 3) Matsumoto, N., Yoshida, H., Sasaki, T., and Annaka, T., Response Spectra of Earthquake Motion at Dam Foundations, Proc. of Twenty-first International Congress on Large Dams (2003)
- 4) Matsumoto, N., Yoshida, H., Sasaki, T., and Annaka, T., "Response Spectra of Earthquake Motions at Dam Sites," Large Dams, No. 186, pp. 69–76, 2004
- 5) Earthquake Research Committee, Headquarters for Earthquake Research Promotion: Appendix: Methods for assessing strong seismic ground motion specifying the causative fault ("recipe"), Strong ground motion assessment on the assumption of the Hyuganada earthquake, http://www.jishin.go.jp/main/kyoshindo/05sep_hyuganada/furoku.pdf, September 2005 (in Japanese)
- 6) Central Disaster Prevention Council, Cabinet Office: Website of the Central Disaster Prevention Council, <http://www.bousai.go.jp/jishin/chubou/index.html> (in Japanese)

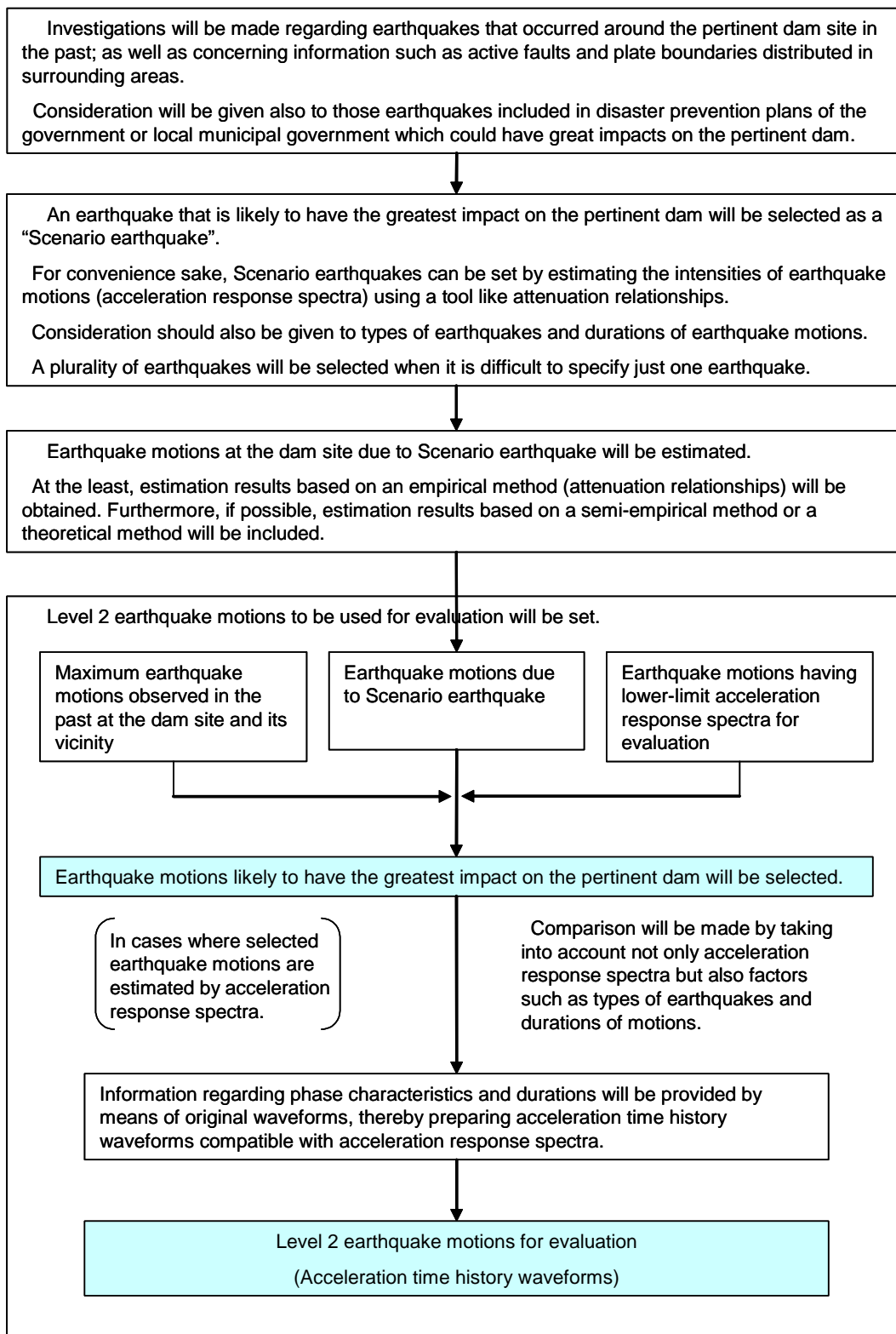
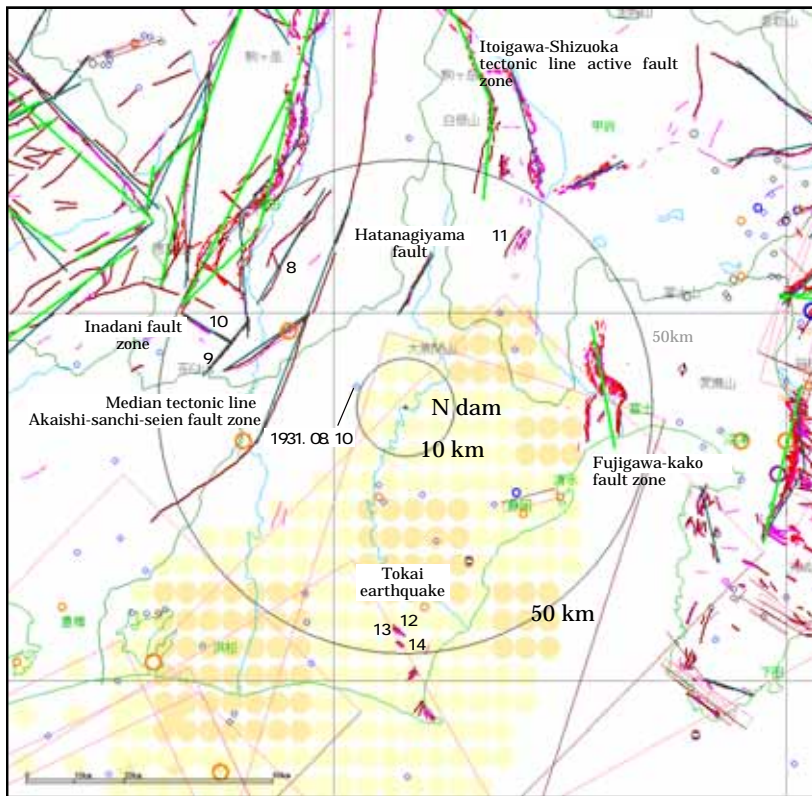
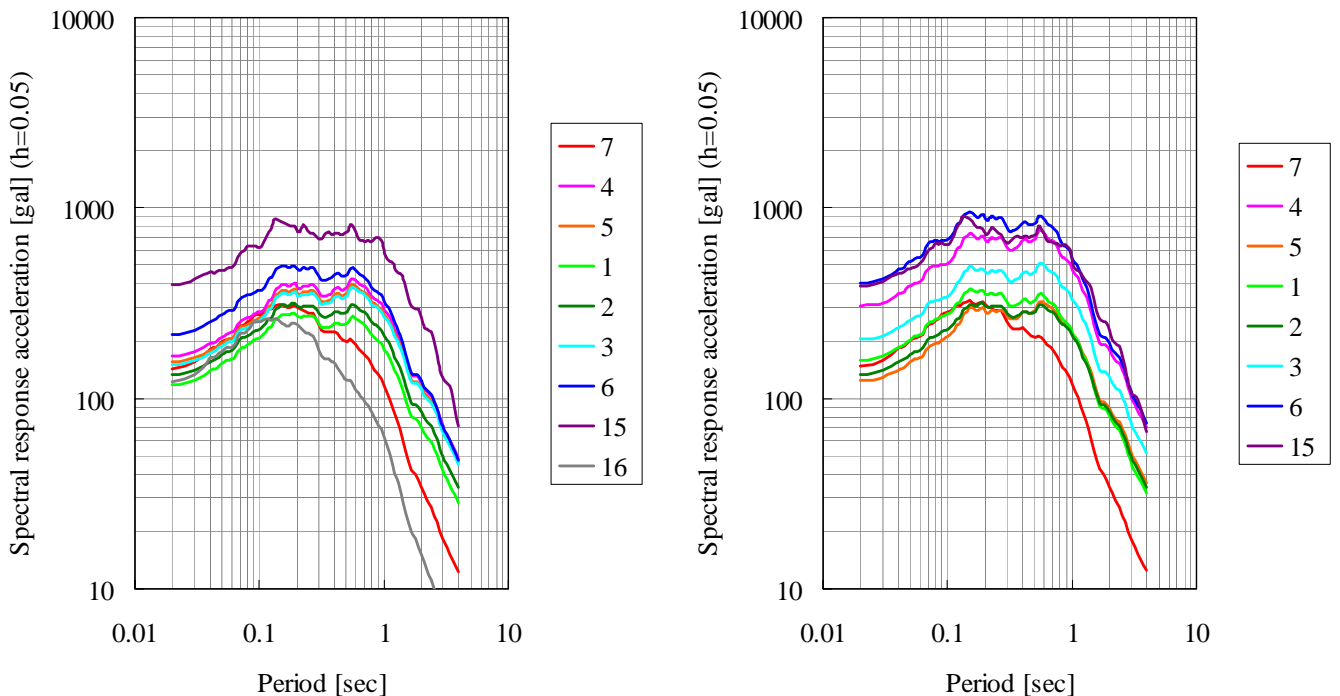


Fig. 1 Flowchart for establishing Level 2 earthquake motions to evaluate seismic performance



No.	Fault
1	Inadani fault zone (fault at the boundary)
2	Inadani fault zone (fault at the toe)
3	Inadani fault zone (throughout the fault zone)
4	Fujigawa-kako fault zone
5	Itoigawa-Shizuoka tectonic line active fault system
6	Median tectonic line Akaishi-sanchi-seien fault zone
7	Hatanagiyama fault
8	Shimoinadaki-higashi fault zone
9	Niino fault
10	Suzugasawa fault
11	Fujimisan fault
12	Niotsuji-higashi fault
13	Niotsuji-nishi fault
14	Maruohara fault
15	Anticipated Tokai earthquake
16	Earthquake of August 10, 1931

Fig. 2 Faults and past earthquakes around N Dam



(a) shortest distance equation (mean + standard deviation)

(b) equivalent distance equation (mean + standard deviation)

Fig. 3 Acceleration response spectra of earthquake motion at N Dam site caused by earthquakes considered in the selection of *Scenario earthquake* (calculated by attenuation relationships)

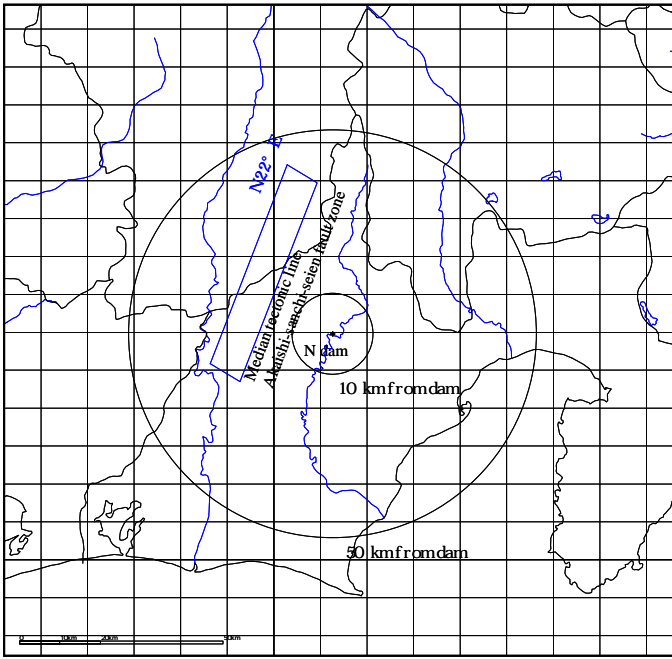


Fig. 4 Location of hypocenter fault model of Scenario earthquake
(Earthquake caused by Akaishi-sanchi-seien fault zone)

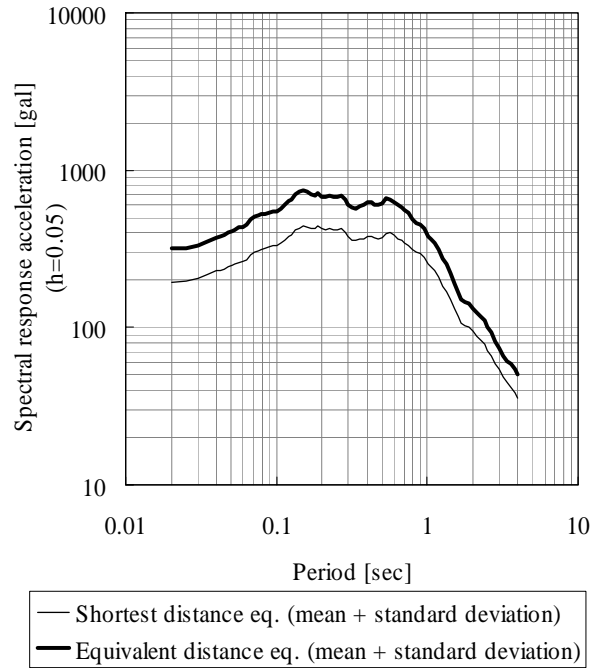
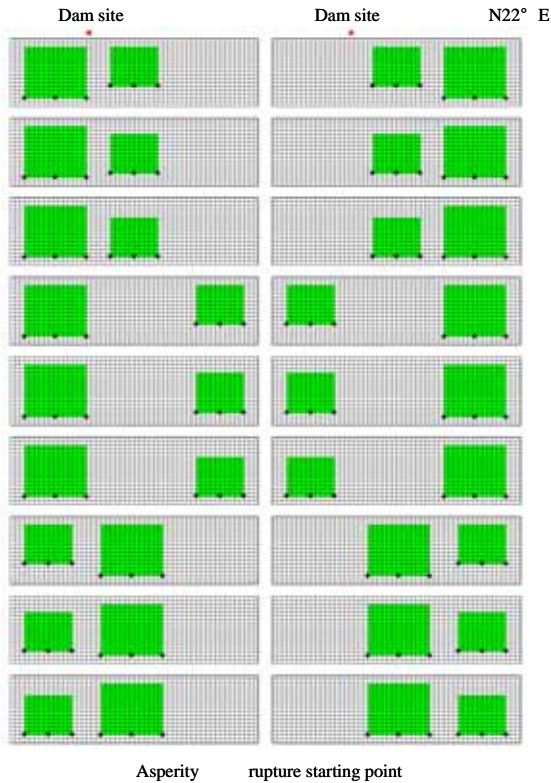


Fig. 5 Acceleration response spectra of earthquake motion at N dam site caused by Scenario earthquake
(Earthquake caused by Akaishi-sanchi-seien fault zone, predicted by attenuation relationships)



Asperity distribution 18 cases × rupture starting point 6 cases = total 108 cases

Fig. 6 Asperity distribution and rupture starting point in hypocenter fault model of Scenario earthquake
(Earthquake caused by Akaishi-sanchi-seien fault zone)

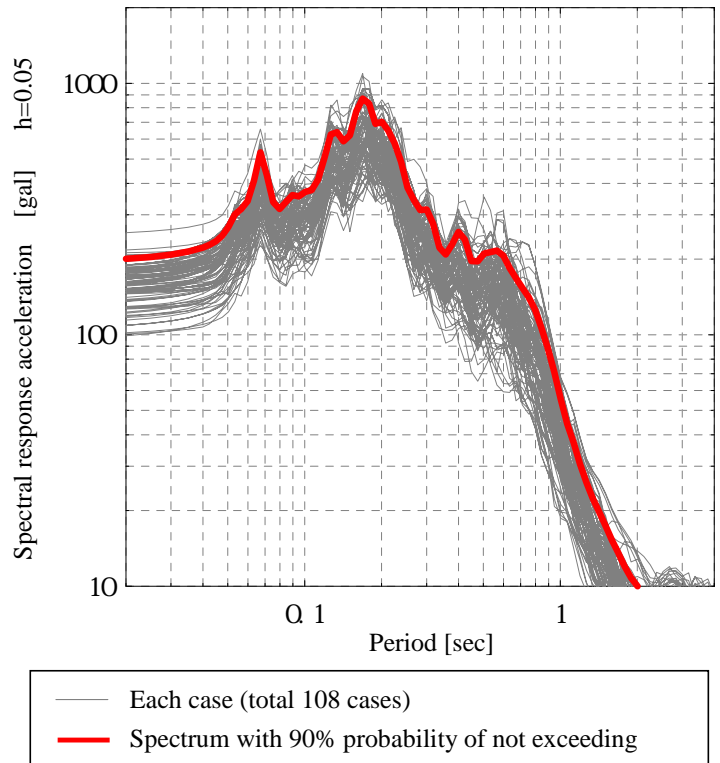


Fig. 7 Acceleration response spectrum of earthquake motion at N dam site caused by Scenario earthquake
(Earthquake caused by Akaishi-sanchi-seien fault zone, predicted by the statistical Green's function method)

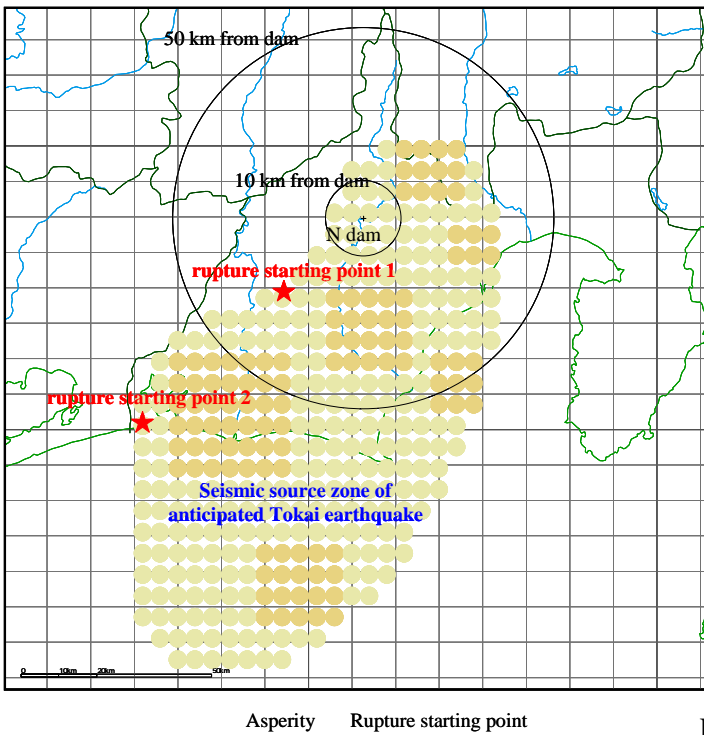


Fig. 8 Location of the hypocenter fault model of Scenario earthquake (Anticipated Tokai Earthquake by Central Disaster Prevention Council)

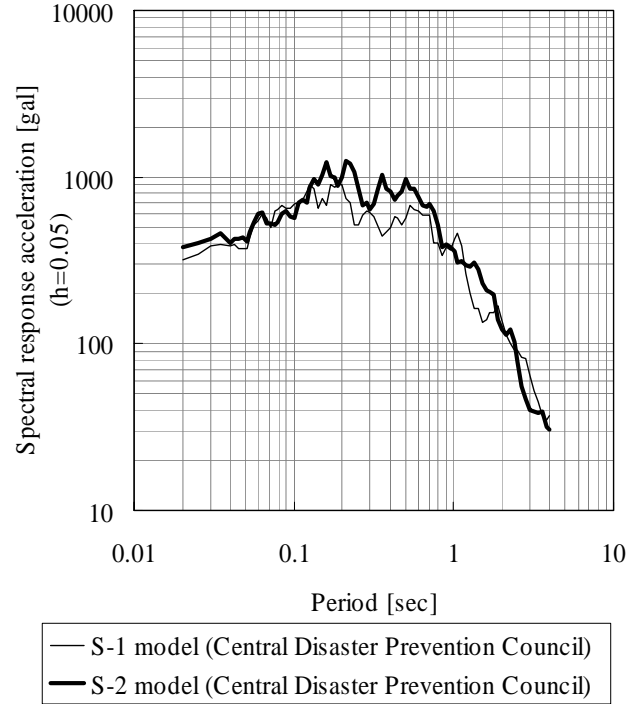


Fig. 9 Acceleration response spectra of earthquake motion at N Dam site caused by Scenario earthquake (Anticipated Tokai Earthquake, predicted by the statistical Green's function method (Central Disaster Prevention Council))

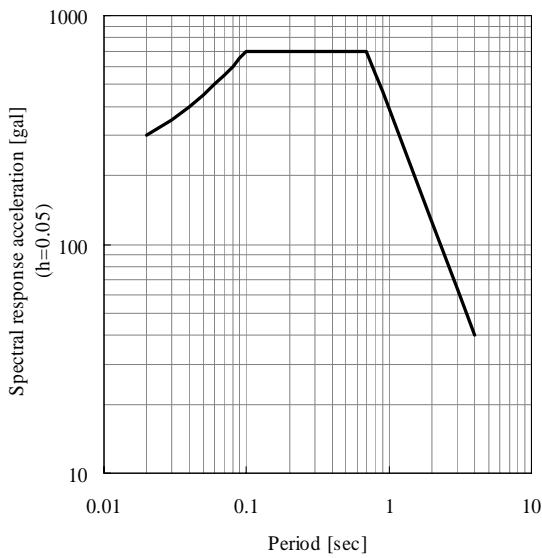


Fig. 10 Lower-limit acceleration response spectra for evaluation

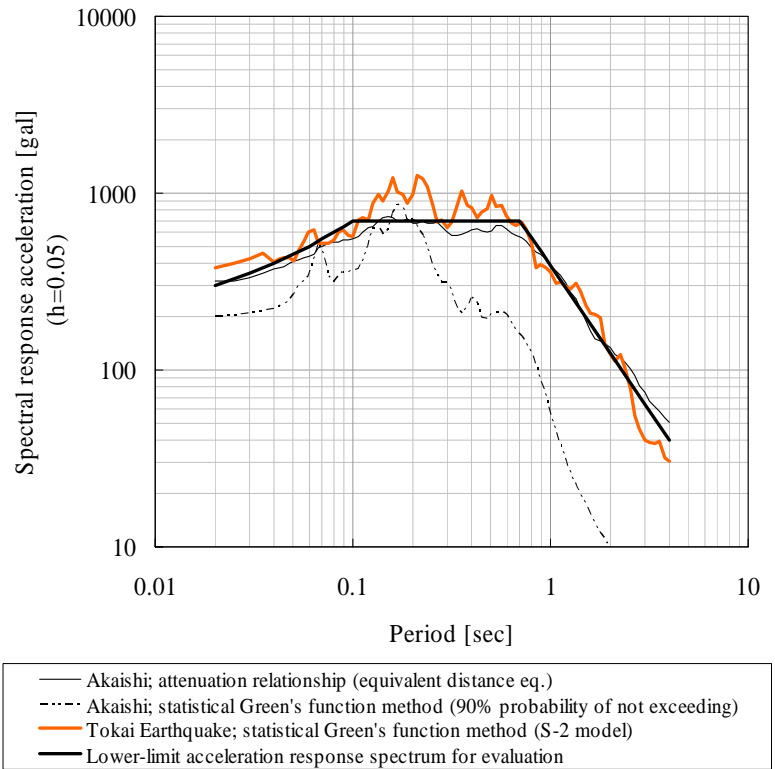
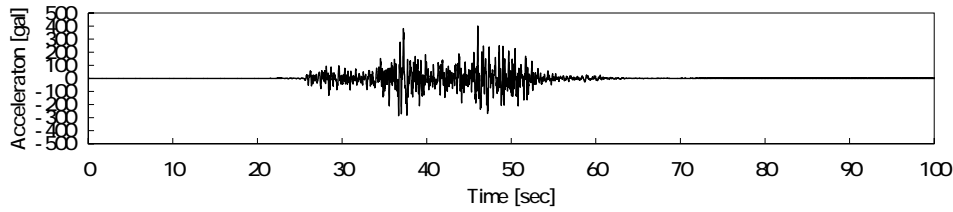
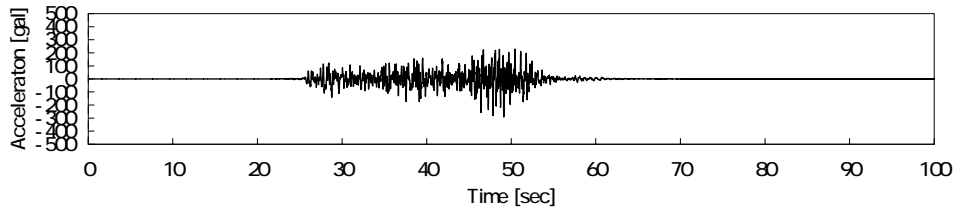


Fig. 11 Acceleration response spectra of earthquake motions at N Dam site caused by Scenario earthquake and lower-limit acceleration response spectra for evaluation

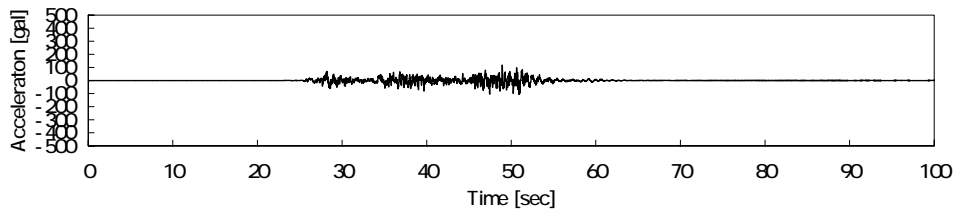
Upstream-downstream direction: maximum amplitude +400.4 [gal]



Dam axis direction: maximum amplitude -297.1 [gal]

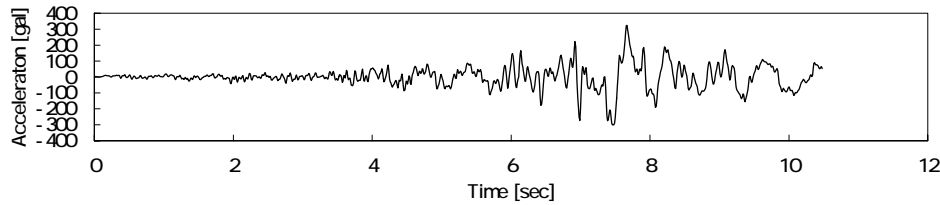


Vertical direction: maximum amplitude +117.8 [gal]

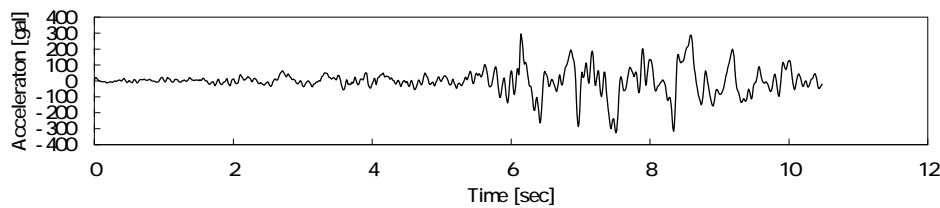


(a) Anticipated Tokai Earthquake (Central Disaster Prevention Council, S-2 model)

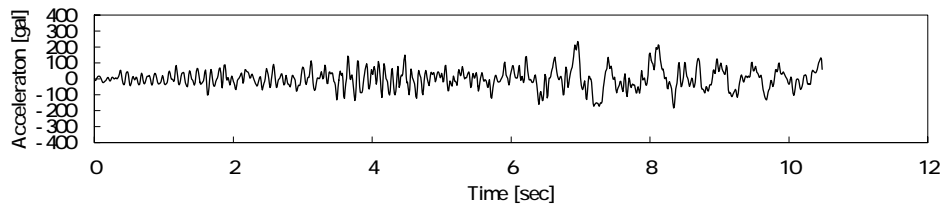
Upstream-downstream direction: maximum amplitude +323.8 [gal]



Dam axis direction: maximum amplitude -326.4 [gal]

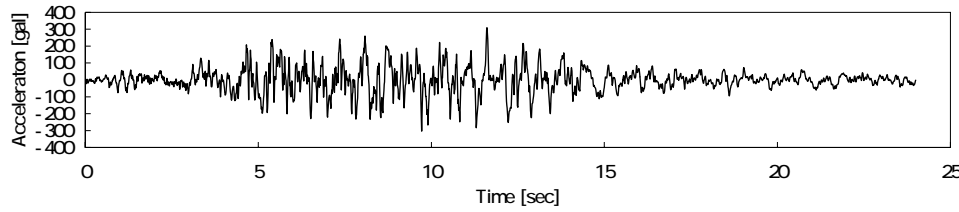


Vertical direction: maximum amplitude +234.6 [gal]

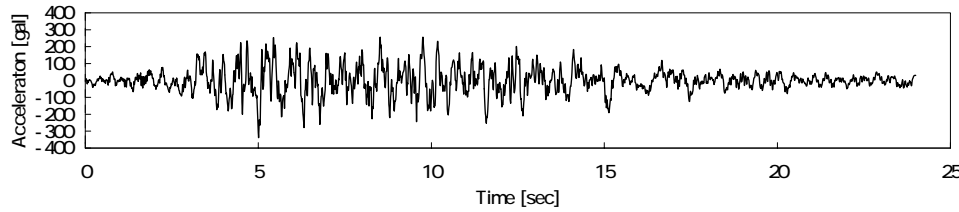


(b) Earthquake motion with lower-limit acceleration response spectra for evaluation
(original waveform: waveform measured at Hitokura Dam during the 1995 Hyogoken-nanbu Earthquake)
Fig. 12 Level 2 earthquake motions used to evaluate seismic performance of N Dam

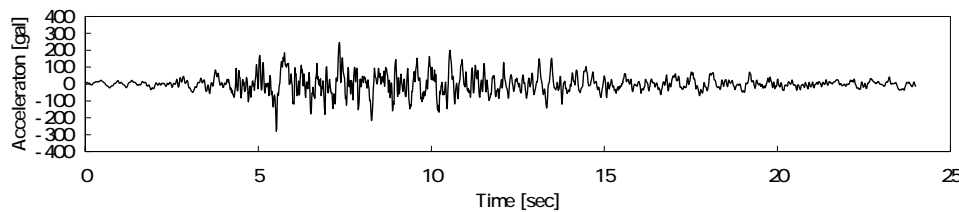
Upstream-downstream direction: maximum amplitude +309.5 [gal]



Dam axis direction: maximum amplitude -338.8 [gal]



Vertical direction: maximum amplitude -280.0 [gal]



(c) Earthquake motion with lower-limit acceleration response spectra for evaluation

(original waveform: waveform measured at Gongen Dam during the 1995 Hyogoken-nanbu Earthquake)
 Fig. 12 Level 2 earthquake motions used to evaluate seismic performance of N Dam

Table 1 Faults and past earthquakes which could affect N Dam

No.	Fault	Fault length	Magnitude	Focus depth	Fault dip	Certainty of existence of the active fault	Activeness	Probability of occurrence	Sources
1	Inadani fault zone (fault at the boundary)	49	7.7	-	NW, W	I	A	7.00%	Headquarters for Earthquake Research Promotion Data on fault dip are from Active Faults in Japan
2	Inadani fault zone (fault at the toe)	57	7.8	-	20 to 40 degrees west ^(*)	I	A	6.00%	Headquarters for Earthquake Research Promotion
3	Inadani fault zone (throughout the fault zone)	78	8.0	-	NW, W	I	A	7.00%	Headquarters for Earthquake Research Promotion Data on fault dip are from Active Faults in Japan
4	Fujigawa-kako fault zone	80	8.0	-	W	I	A	11.00%	Headquarters for Earthquake Research Promotion Data on fault dip are from Active Faults in Japan
5	Itoigawa-Shizuoka tectonic line active fault system	150	8.0	-	Westward dip (in the south)	I	A	14.00%	Headquarters for Earthquake Research Promotion (No data available on turning points)
6	Median tectonic line Akaishi-sanchi-seien fault zone	52	7.8	-	S, E	I	B	-	Headquarters for Earthquake Research Promotion Data on fault dip are from Active Faults in Japan
7	Hatanagiyama fault	14	6.7	-	E	II	C	-	Matsuda (2000) Data on fault dip are from Active Faults in Japan
8	Shimoinadaki-higashi fault zone	27	7.2	-	E	II	B	-	Matsuda (2000) Data on fault dip are from Active Faults in Japan
9	Niino fault	14	6.7	-	E or W	II	B ~ C	-	Matsuda (2000) Data on fault dip are from Active Faults in Japan
10	Suzugasawa fault	10	6.5	-	S	I	B	-	Matsuda (2000) Data on fault dip are from Active Faults in Japan
11	Fujimisan fault	7	6.2	-	W	I	C	-	Active Faults in Japan Magnitude was calculated by Matsuda's equation
12	Niotsuji-higashi fault	3	5.6	-	SW or NE	I	B ~ C	-	Active Faults in Japan Magnitude was calculated by Matsuda's equation
13	Niotsuji-nishi fault	2	5.3	-	SW	I	C	-	Active Faults in Japan Magnitude was calculated by Matsuda's equation
14	Maruhara fault	2	5.3	-	S	I	C	-	Active Faults in Japan Magnitude was calculated by Matsuda's equation
15	Anticipated Tokai earthquake	-	7.7	-	NW	-	-	-	Central Disaster Prevention Council
16	Earthquake of August 10, 1931	-	5.9	0.0	-	-	-	-	Japan Meteorological Agency's annual seismic report (latest data are available)

(*) shallower than 150 to 300 m below ground surface

Table 2 Parameters on fault of Scenario earthquake and attenuation relationships
(Median tectonic line Akaishi-sanchi-seien fault zone, used in attenuation relationships)

(a) Parameters used in attenuation relationships

Dam site	Fault/earthquake	Type of focus	Japan Meteorological Agency magnitude	Shortest distance to fault (km)	Equivalent epicentral distance (km)	Depth of the center of fault plane (km)
N Dam	Median tectonic line Akaishi-sanchi-seien fault zone	Shallow crustal	7.6	23.9	28.5	10.5

(b) Parameters on the hypocenter fault

Japan Meteorological Agency magnitude	Fault length [km]	Fault width [km]	Fault area [km ²]	Dip [deg]	Depth of upper edge [km]	Depth of lower edge [km]
7.6	52	17	884	60	3	18

Table 3 Parameters on the hypocenter fault of Scenario earthquake
(Median tectonic line Akaishi-sanchi-seien fault zone, used for the statistical Green's function method)

Characteristics of focus		Specified value	Source
Macro characteristics of focus	Latitude	137.82 [deg]	Report of the Headquarters for Earthquake Research Promotion
	Longitude	35.10 [deg]	Report of the Headquarters for Earthquake Research Promotion
	Strike	22 [deg]	Report of the Headquarters for Earthquake Research Promotion
	Dip	60 [deg]	
	Length L	52 [km]	Report of the Headquarters for Earthquake Research Promotion
	Width W	17 [km]	$W=(H_a-H_b)/\sin\alpha$
	Depth of the top edge of the fault below the ground surface d	3 [km]	Report of the Headquarters for Earthquake Research Promotion
	Fault area S	884 [km ²]	$S=LW$
	Reduction of static stress	4.03 [MPa]	Boatwrite (1988)
	Seismic moment M_0	4.35E+19 [Nm]	Wells and Coppersmith (1994) $S=4.24 \times 10^{-11} M_0^{1/2}$
	Moment magnitude M_w	7.03	Kanamori (1977) $\log M_0=1.5M_w+9.1$
	Secondary wave velocity V_s	3.46 [km/s]	
	Density	2.70 [g/cm ³]	
	Rigidity μ	3.23E+10 [N/m ²]	$\mu=rV_s^2$
	Mean slippage D	1.5 [m]	$M_0=r \cdot D \cdot S$
Short period level of entire fault A	1.86E+19 [Nm/s ²]	Dan et al. (2001) $A=2.46 \times 10^{17} M_0^{1/3}$	
Micro characteristics of focus	Entire asperity	Area of entire asperity S_a	263 [km ²] Boatwright (1988), Dan et al. (2001) $S_a=r^2 \quad r=(7p/4) \times M_0/(A \cdot R) \cdot V_s^2$
		Mean slippage of entire asperity D_a	3.0 [m] Somerville et al. (1999) $D_a=D \times 2$
		Seismic moment of entire asperity M_{0a}	2.59E+19 [Nm] $M_{0a}=m \cdot D_a \cdot S_a$
		Reduction of static stress of asperity a	13.53 [MPa] Madariaga (1979) $DS_a=(S/S_a) \cdot D_s$
	First asperity	Area of asperity S_{a1}	175 [km ²]
		Mean slippage of asperity D_{a1}	3.4 [m] $D_{a1}=(g_1/Sg_1^3) \cdot D_a$
		Seismic moment of asperity M_{0a1}	1.91E+19 [Nm] $M_{0a1}=m \cdot D_{a1} \cdot S_{a1}$
		Effective stress of asperity s_{a1}	13.53 [MPa] $s_{a1}=DS_a$
	Second asperity	Area of asperity S_{a2}	88 [km ²]
		Mean slippage of asperity D_{a2}	2.4 [m] $D_{a2}=(g_2/Sg_2^3) \cdot D_a$
		Seismic moment of asperity M_{0a2}	6.76E+18 [Nm] $M_{0a2}=m \cdot D_{a2} \cdot S_{a2}$
		Effective stress of asperity s_{a2}	13.53 [MPa] $s_{a2}=DS_a$
Background	Background area S_b	621 [km ²] $S_b=S-S_a$	
	Mean slippage in the background D_b	0.9 [m] $M_{0b}=m \cdot D_b \cdot S_b$	
	Seismic moment of the background M_{0b}	1.76E+19 [Nm] $M_{0b}=M_0-M_{0a}$	
	Effective stress of the background s_b	2.74 [MPa] Dan et al. (2002) $s_b=(D_b/W_b) \cdot (p^{1/2}/D_a) \cdot r \cdot Sg_1^3 \cdot s_a$	
Other characteristics of focus	Rupture propagation velocity V_r	2.77 [km/s]	Kataoka et al. (2003) $V_r=0.8 \cdot V_s$
	Rise time of first asperity tr_{a1}	1.20 [s]	Nakamura and Miyatake (2000), Kataoka et al. (2003) $tr=0.25 \cdot W/V_r$
	Rise time of second asperity tr_{a2}	0.85 [s]	
	Rise time of the background tr_b	1.54 [s]	
	High frequency cutoff f_{max}	6.0 [Hz]	Tsurugi (1997)